2

Adaptive Fractional Fourier Domain Filtering in Active Noise Control

Sultan Aldırmaz and Lütfiye Durak–Ata
Department of Electronics and Communications Engineering, Yildiz Technical University
Turkey

1. Introduction

Acoustic noise control systems gain more importance as more and more industrial equipments, i.e., engines, fans, ventilators, and exhausters are in use (1–6). Passive acoustic noise control techniques benefit enclosures, barriers and silencers to attenuate ambient noise. However, if the noise has dominant low-frequency components, then passive techniques are either inefficient or expensive. In contrast, active noise control (ANC) systems are much more effective in canceling low-frequency noise. Various noise cancelation algorithms have been proposed in the literature (7–11). In a generic ANC scheme, a reference microphone is used to receive the ambient noise and the system produces an *anti-noise* signal which has equal amplitude but opposite phase with the primary noise to cancel it acoustically (1). As the primary noise may have time-varying characteristics, ANC systems should be able to adapt themselves to the noise rapidly.

In most of the ANC systems, either adaptive filters or neural network based structures are employed (2–6; 9; 12–18). In (15), fuzzy-neural networks are used to estimate the nonlinear response of the unknown primary acoustic path where primary and secondary paths are characterized by nonlinear functions. On the other hand adaptive filters are usually employed to increase the system performance and robustness. They are mostly employed with least mean squares (LMS)-based algorithms and the adaptation is usually realized in time domain (3; 9; 12; 13; 19). Whereas Fourier domain (20) and wavelet-based adaptive filter bank approaches (21; 22) are among the few transform-domain adaptation techniques that have been used in the ANC systems. Compared to time-domain adaptive filters, transform-domain adaptive filters may need fewer parameters (23; 24). When the noise source has dominant low-frequency components, wavelet transform-based adaptive filters provide higher performance rates. However, in case of linear frequency modulated (LFM) or chirp-type audio signals, as their frequency varies linearly with time, performance rates are limited for both Fourier and wavelet-transform domains.

LFM signals are among the frequently used signals in real life and they are good models for mechanical systems with accelerating internal components. A Gaussian enveloped,

[1] The authors are supported by the Scientific and Technological Research Council of Turkey, TUBITAK under the grant of Project No. 105E078.

[2] The material in this chapter was published in part at [33].

single-component LFM signal can be expressed as

$$x(t) = A\, e^{\pi\gamma(t-t_0)^2}\, e^{j\pi[\alpha(t-t_0)^2+2\beta(t-t_0)]} \tag{1}$$

where α is the chirp rate, t_0 and β represent the time and frequency shifts with respect to the time-frequency origin, A and γ are the parameters of the envelope. One of the most convenient analysis tools for LFM signals is the fractional Fourier transform (FrFT), which employs chirps as basis functions. FrFT is a generalization of the ordinary Fourier transform with a fractional order parameter. It is a mathematically powerful and efficiently computable linear transform. It has been employed in various application areas including time-frequency signal processing, filtering, and denoising (25). Recently, the authors have introduced the adaptive filtering scheme in fractional Fourier domain in (33).

In this chapter, we present a robust adaptive fractional Fourier domain filtering scheme in the presence of LFM signals and additive white Gaussian noise (AWGN). As the instantaneous frequency (IF) of LFM signals may show rapid variations in time, adaptation to a chirp signal is much more difficult compared to a sinusoidal signal in ANC systems. As a remedy to this problem, we propose to incorporate the FrFT.

Adaptive fractional Fourier domain filtering introduces significant improvements, since chirp-type signals are transformed into narrow-band sinusoidal signals and the non-stationary signal adaptation problem is converted to a stationary form. To improve the system performance, it is necessary to estimate the transformation order of FrFT successfully. This is directly related to the proper estimation of the IF of the chirp signal and the estimation should be kept up-to-date at certain time intervals. Many methods are proposed for IF estimation in the literature, such as polynomial phase-based estimators, LMS or RLS-based adaptive filters, and time-frequency distribution-based estimators with same inherent disadvantages (31; 32). Here IF is determined by exploiting the relationship between the Radon-Wigner transform (RWT) and FrFT of signals (29).

The chapter is organized as follows. Section 2 introduces the preliminaries of the chapter by introducing the FrFT giving its definition, important properties and its fast computation algorithm. Then, the IF estimation of single or multi–component LFM signals are investigated. Time and Fourier domain adaptive filtering schemes are explained in Section 3. In Section 4, the ANC system model, FrFT-based adaptation scheme and its performance analysis are given in detail. Finally the conclusions are drawn in Section 5.

Keywords
Active Noise Control, Adaptive filtering, Fractional Fourier transform, Fractional Fourier domains, Instantaneous frequency estimation.

2. Preliminaries

2.1 Fractional Fourier transform

FrFT is a generalization of the ordinary Fourier transform with a fractional order parameter a, which corresponds to the a^{th} fractional power of the Fourier transform operator, $\mathfrak{F}$. The a^{th}-order FrFT of $x(t)$ is defined as

$$x_a = \mathfrak{F}_a\{x(t)\} = \int K_a(t,t')x(t')dt' \tag{2}$$

where $0 < |a| < 2$, and the transformation kernel $K_a(t, t')$ is

$$K_a(t,t') = A_\varphi e^{-j\pi(t2\cot(\varphi) - 2tt'\csc(\varphi) + t'2\cot(\varphi)} \\ A_\varphi = e^{-j\pi sgn(\sin(\varphi))/4 + j(\varphi)/2} / |\sin(\varphi)|^{1/2} \tag{3}$$

with the transform angle $\varphi = a\pi/2$ (25). The first–order FrFT is the ordinary Fourier transform and the zeroth-order FrFT is the identity transformation. The a^{th}-order FrFT interpolates between the function $x(t)$ and its Fourier transform $X(f)$. Fig. 1 shows the real part of a mono–component LFM signal $x(t)$ with a chirp rate $\alpha = 0.5$ in various fractional orders. Time domain signal, i.e. the zeroth–order FrFT, is given in Fig. 1 (a) and its Fourier transform is given in Fig. 1 (c). Moreover, Fig. 1 (b) and (d) show the signal in 0.5^{th} and 1.5^{th} order fractional domains.

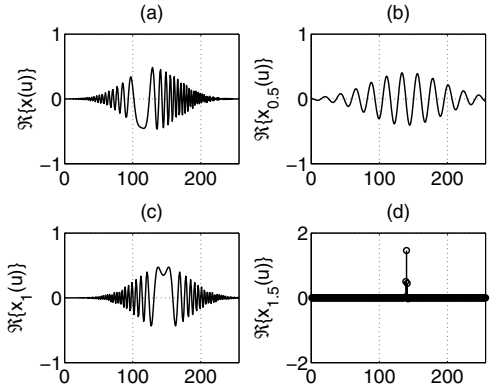

Fig. 1. The real part of the FrFT of the mono-component LFM signal in various fractional orders. (a) The signal in time domain, (b) 0.5^{th} order FrFT, (c) 1^{st} order FrFT, i.e. the Fourier transform, and (d) 1.5^{th} order FrFT.

The inverse transform operator is simply expressed as $(\mathfrak{F}_a)^{-1} = \mathfrak{F}_{-a}$ which corresponds to $K_a^{-1}(t,t') = K_{-a}(t,t')$ as the inverse-transform kernel function. FrFT is a linear and unitary transform. One of the important properties of the FrFT is index additivity and it is expressed as

$$\mathfrak{F}_{a_1}\mathfrak{F}_{a_2} = \mathfrak{F}_{a_1+a_2} \tag{4}$$

where a_1 and a_2 indicate the fractional transform orders.
In (26), FrFT is decomposed into a chirp multiplication followed by a chirp convolution and followed by another chirp multiplication. The chirp convolution is evaluated by using the fast Fourier transform. Thus, FrFT can be computed by $O(N\log N)$ computational complexity, where N denotes the time–bandwidth product (TBP) of the signal (26). The TBP of a signal *x(.)* is defined as the product of time–width and bandwidth of the signal. According to the well-known uncertainty principle, signals can not be confined both in time and frequency at the same time. However, it is always possible to choose the TBP of the signal large (always greater than 1). Therefore, authors in (26) assumed that the signal is confined to the interval $[-\Delta t/2, \Delta t/2]$ in time and $[-\Delta f/2, \Delta f/2]$ in frequency domain. In order to have same length of time and frequency interval, a scaling operator must be used. When time domain scaling

$c_1[m] := e^{J\pi\frac{1}{4}(\alpha/dx^2-\beta/N)m^2}$	$-N \le m \le N-1$
$c_2[m] := e^{J\pi\beta(m/2\sqrt{N})^2}$	$-2N \le m \le 2N-1$
$c_3[m] := e^{J\pi\frac{dx^2}{4N}(\alpha/N-\beta/dx^2)m^2}$	$-N \le m \le N-1$
$g[m] := c_1[m]x(m/2dx)$	$-N \le m \le N-1$
$h_{a'}(m/2dx) := \frac{A_\phi}{2dx}c_3[m](c_2 * g)[m]$	$-N \le m \le N-1$

where,
$\phi'' := \frac{\pi}{2}a''$
$\alpha := \cot\phi''$
$\beta := \csc\phi''$
$A_\phi := \frac{exp(-j\pi\mathrm{sgn}(\sin\phi)/4+j\phi/2)}{|\sin\phi|^{1/2}}$

Table 1. Table 1. Definition of the variables in Fig.2, which are used in the calculation of the fast fractional Fourier transform algorithm

is employed to the signal, time and frequency axes become $\Delta t/s$ and Δfs, respectively. By defining the scale parameter as $s = \sqrt{\Delta t/\Delta f}$, new time and frequency axis (range, interval) become same and it is $\Delta x = \sqrt{\Delta f \Delta t}$. Therefore the TBP is $N = \Delta t \Delta f$, the interval of the samples is defined in terms of the TBP, $\Delta x = \sqrt{N}$.
The fast FrFT computation block diagram is given in Fig. 2. First, the signal is interpolated by 2, then the interpolated signal is multiplied by a chirp signal c_1. After then, the obtained signal is convolved by a chirp c_2 and multiplied another chirp c_3. Finally, the obtained signal is downsampled by 2. In the algorithm, the fractional transform order, a, is assumed to be in the interval $0.5 \le |a| \le 1.5$. The index additivity property of the FrFT can be used to extend this range.
As mentioned in the next section, FrFT has some impacts on the Wigner distribution (WD). Roughly speaking, FrFT rotates the support of the signal on the x-y axis respect to the transform order. In order to preserve the energy of the signal in a circle with a Δx diameter, the analyzed signal must be interpolated by 2 times in the beginning of the algorithm. (26) presents the digital computation of the FrFT, moreover, discrete FrFT definitions have been developed by many researchers (27; 28).

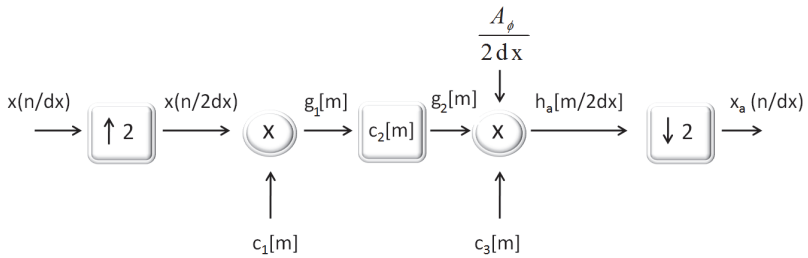

Fig. 2. The fast FrFT computation block diagram.

2.2 IF estimation of chirp-type signals

FrFT converts time-varying chirp-type signals into sinusoidals at appropriate transform orders. Thus it is crucial to estimate the instantaneous frequency (IF) value of the chirp components successfully. The IFs of the analyzed signals characterize the variation of their spectra.

The WD of a signal $x(t)$ is represented by $W_x(t,f)$ and defined as

$$W_x(t,f) = \int x(t+\tau/2)x^*(t-\tau/2)e^{-j2\pi f\tau}d\tau. \tag{5}$$

The RWT of a signal $x(t)$ is defined as the Radon transform of the WD of $x(t)$,

$$RDN[W_x](r,\varphi) = \int W_x(r\cos(\varphi)-s\sin(\varphi), r\sin(\varphi)+s\cos(\varphi))ds \tag{6}$$

where (r,φ) are the transform-domain variables in polar coordinates and the RWT gives the projection of the WD for $0 \leq \varphi \leq \pi$. The radial slices of the RWT, $RDN[W_x](r,\varphi)$, can be directly computed from the FrFT of the signal as,

$$RDN[W_x](r,\varphi) = |\mathfrak{F}_a\{x(r)\}|^2 = |x_a(r)|^2\,. \tag{7}$$

A mono-component amplitude-modulated chirp signal and its time-frequency representation by WD are shown in Fig. 3(a) and (b). FrFT rotates the WD of the signal by an angle related to the fractional transformation angle φ, as shown in Fig. 3 (c) and (d). The appropriate order of the FrFT, which is $(1/3)$ for this case, rotates the WD in the clockwise direction so that the chirp is converted to an amplitude modulated sinusoidal signal.

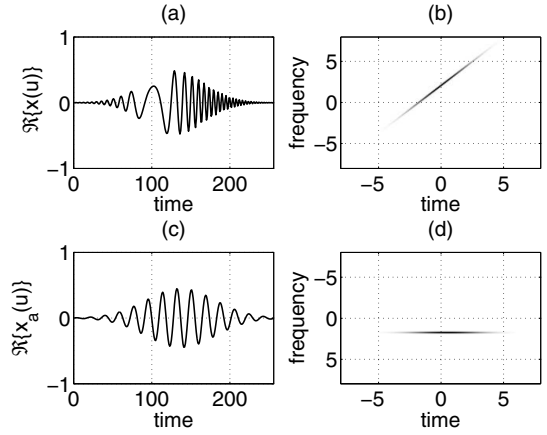

Fig. 3. (a) Real part of the LFM signal in time-domain, (b) its WD, (c) its (1/3)-rd order FrFT, and (d) the WD of the transformed signal.

The projections in the WD domain are related to the FrFT and we propose an efficient and a simple IF estimation technique by using the relationship between the RWT of a signal and its corresponding FrFT (29). The algorithm searches for the appropriate FrFT order a for the signal. At the appropriate order, FrFT of the signal gives the maximum peak value. By

searching the peaks of $|x_a(r)|^2$ computed in $O(N\log N)$ operations at various order parameter values of $0 < |a| < 2$, the LFM rates and IF estimates can be determined robustly.

As the a^{th}-order FrFT gives $x(t)$ for $a = 0$ and $X(f)$ for $a = 1$, binary search algorithm searches for the optimum transformation order between zero and one that maximizes the peak FrFT value. First, this algorithm calculates the FrFT of the signal for $a = 0$, $a = 0.5$, and $a = 1$ values. Secondly, it takes the maximum two peak values of the FrFT among these values. Then, FrFT calculation is repeated for two obtained peak values and their mean value. This procedure is iteratively repeated by decreasing the search region for the order parameter a. The flowchart of this algorithm is given in Fig. 4. As each FrFT computation has *O(NlogN)* complexity, the overall complexity of the required search is of *O(3x L x N(logN))*, where L indicates the loop number of the search algorithm and 10 steps is usually sufficient.

Such an RWT-based IF estimation works well even the environment has AWGN besides the chirp-type noise. The peak FrFT value of the chirp signal in Fig. 5 with respect to the FrFT order $(a - 1)$ is presented for AWGN with three different SNR values.

If the signal has multi–chirp components, then each peak belonging to each different IF should be determined. For a multi–component chirp signal, Fig. 6 shows peak FrFT values of each component. Chirp rate of these components are $[\pi/18, \quad 2\pi/9, \quad 3\pi/12]$ and their time and frequency centers are $t_0 = [0, \quad 0, \quad 1]$ and $b = [-1, \quad 0, \quad 1]$, respectively. Although this technique works for the multiÚcomponent case, its performance depends on the SNR value and difference between IF values of each component of the analyzed signal. For this reason, if the ambient noise has more than one component, the minimum-essential-bandwidth-based IF estimation technique can be used as in (28).

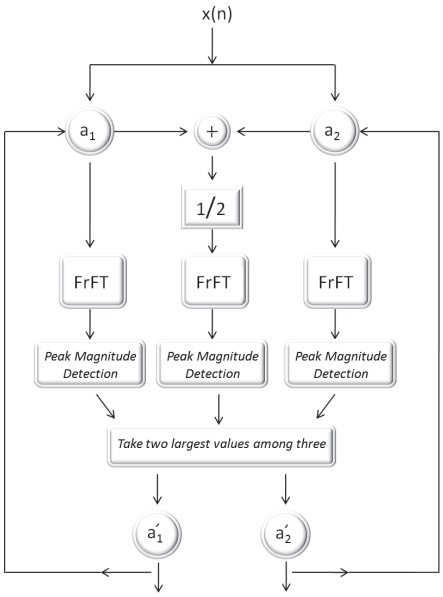

Fig. 4. A basic IF estimation scheme via RWT.

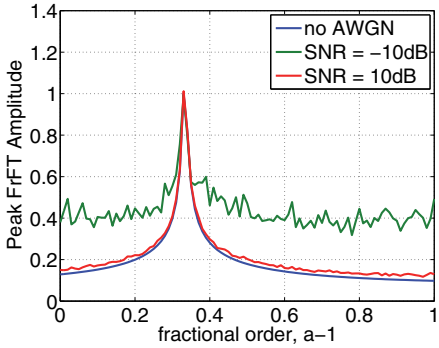

Fig. 5. Peak FrFT values as a function of the fractional order, (a-1) for a mono–component chirp signal.

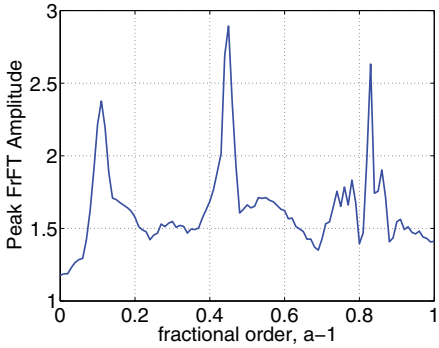

Fig. 6. Peak FrFT values as a function of the fractional order, (a-1) for multi–component chirp signal.

(28) shows that the fractional Fourier domain order corresponding to the transformed signal of minimum bandwidth gives IF estimates in sufficiently long observation periods for multiŰcomponent signals. In (28), two different IF estimation algorithms are proposed in that optimization scheme. One of them makes use of the maximum fractional time-bandwidth ratio, whereas the second one introduces a minimum essential bandwidth, which is expressed as the minimum sum of the bandwidths of the separate signal components. Genetic algorithm is employed to determine the IF of the signal components.

3. Adaptive filtering in ANC systems

Most of the ANC systems employ adaptive filters based on LMS-type algorithms, operating either in time or transform domains. In some applications, such as acoustic echo cancellation in teleconferencing, time-domain adaptive filters should have long impulse responses in order to cancel long echoes successfully. On the other hand, transform-domain adaptive filters may converge faster than time-domain adaptive filters in such cases.

We propose a fractional Fourier domain adaptive filtering scheme for ANC systems as given in Fig. 7. The effect of the environment is summarized by an unknown plant *P(z)* from

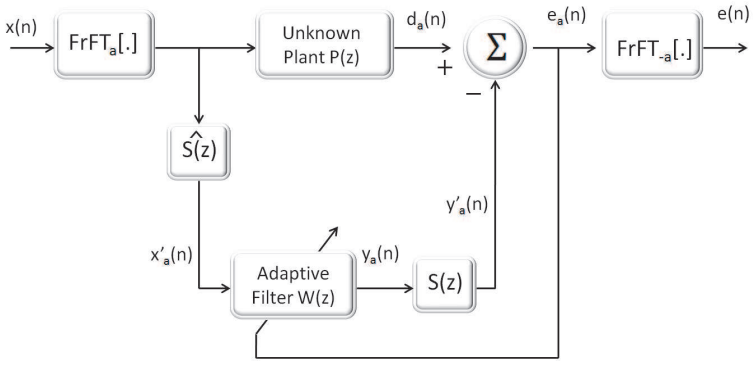

Fig. 7. The basic scheme of the FrFT-domain adaptive filter in an ANC application.

the reference microphone to the error microphone. Secondary path from the canceling loudspeaker to the error microphone is represented by $S(z)$. Secondary path effects include the effect of power amplifiers, microphones, speakers, analog-to-digital converters and digital-to-analog converters. In (19), secondary path transfer functions have been estimated, whereas in (4; 14), the secondary path is modeled as an FIR filter. (34) emphasizes on the system identification problem of ANC, thus the secondary path is not considered. Here, we employ a secondary acoustic path model as an FIR filter and assume its proper estimation as $\hat{S}(z)$, and we focus on the fractional Fourier domain adaptive filtering scheme.

3.1 Time-domain adaptation

Searching the optimum filter tap-weights to minimize the sums of squares of the cumulative error, LMS-based algorithms achieve satisfactory performance rates with low computational complexity. Assuming that $\mathbf{x}_p(n)$ is the input vector at time n, instantaneous error of the adaptive filter is

$$e(n) = d(n) - s(n)[\mathbf{w}^T(n)\mathbf{x}'_p(n)] \tag{8}$$

where $e(n)$, $d(n)$ and $\mathbf{w}(n)$ denote the error signal, reference signal, and the adaptive filter tap-weights, respectively. Error is minimized by decreasing the filter tap-weights in the direction of the gradient with a step-size μ recursively

$$\mathbf{w}(n+1) = \mathbf{w}(n) + \mu\mathbf{x}_p(n)e^*(n). \tag{9}$$

To reduce the effect of the power of the input signal on the system performance μ may be normalized by the power of the signal as in the normalized-LMS (NLMS) algorithm.
In ANC systems, filtered-X LMS (Fx-LMS) algorithm is used to reduce the secondary path effects. In the Fx-LMS algorithm, tap-weights $\mathbf{w}(n)$ are recursively adapted in the direction

[3] In this section, lowercase boldface italic characters generally refer to vectors and (.)* is used to denote the Hermitian conjugate operation for matrices.

of the gradient with a step-size μ by using the filtered reference signal through the secondary path model $s(n)$,

$$\mathbf{w}(n+1) = \mathbf{w}(n) + \mu \mathbf{x}'_p(n) e^*(n) \tag{10}$$

where $\mathbf{x}'_p$ is the filtered $\mathbf{x}_p$.
A summary of the Fx-LMS algorithm is given in Table 2. Time-domain adaptation to a chirp signal is presented in Fig. 11 where the reference signal is $d(n)$ and the corresponding output of the time-domain LMS-based adaptive filter is $y(n)$. The error increases as the frequency of the input signal changes rapidly. The performance of the adaptive filtering scheme is also investigated by using the NLMS algorithm. The error signal $e(n)$, of the LMS-based adaptive filter in time-domain is illustrated in Fig. 11 (a), whereas the error signal of the NLMS-based adaptive filter in the time domain is shown in Fig. 11 (b).

3.2 Fourier–domain adaptation

Fourier–domain adaptation improves the adaptive filter performance for several reasons. For example, time domain adaptation requires the convolution operation and when the impulse response gets long, the overall complexity increases. By using fast Fourier transform, the computational complexity can be reduced, which is one of the reasons in choosing Fourier domain adaptation. The other reason is that frequency domain adaptive filtering improves the convergence performance. Moreover, orthogonality properties of the discrete Fourier transform provides a more uniform convergence rate (24).

4. System model and simulations

The adaptive LMS-based ANC system in fractional Fourier domain is designed as shown in Fig 8. An adaptive filter is used to model the primary path effect *P(z)*, which is the acoustic response from the reference sensor to the error sensor. Reference signal is obtained by measuring the ambient noise and the primary signal is the output of the unknown plant. The ambient noise that shows chirp-type characteristics is modeled by an adaptive filter in fractional Fourier domain which transforms non-stationary chirp-type signals to stationary sinusoidal signals. The acoustic anti-noise signal, which is the inverse-FrFT of the adaptive filter output, is generated by the loudspeaker. Except the FrFT-order estimation at certain time intervals, adaptation scheme is the same as the Fourier-domain adaptation in practical circuits and systems applications. A chirp-type noise signal to be modeled by the fractional Fourier domain adaptive filter and its appropriately-ordered FrFT are shown in Fig. 9(a) and (b). The chirp signal is transformed to a sinusoidal signal at the estimated transformation order of $a = 1/3$ by the proposed binary search algorithm. The input and output signals of the LMS-based adaptive filter in the fractional Fourier domain are given in Fig. 9(b) and (c). By taking the inverse FrFT of (c), time-domain filter output is obtained as shown in (d). The fractional Fourier domain error signals of both LMS and NLMS-based adaptive filters are plotted in Fig. 10(a) and (b). Among the two algorithms, NLMS performed better. Moreover, the corresponding time-domain error signals of the fractional Fourier domain adaptive filters by LMS and NLMS algorithms are presented in Fig. 11(a) and (b). Compared to the error plots of time-domain adaptation in Fig. 4(b) and 5(b), the fractional Fourier domain adaptive filtering scheme achieves significantly better performance. Finally, the performance of the adaptive fractional Fourier domain LMS-based ANC is tested when the chirp-type noise

signal is embedded into AWGN. Fig. 12 presents error energy with respect to SNR, e.g., when SNR is 8 dB, the error energy in fractional Fourier domain adaptation scheme is less than 10^{-1}, whereas if the adaptation is realized in time, the error energy is greater than 1. Fractional Fourier domain adaptation noticeably improves the system performance.

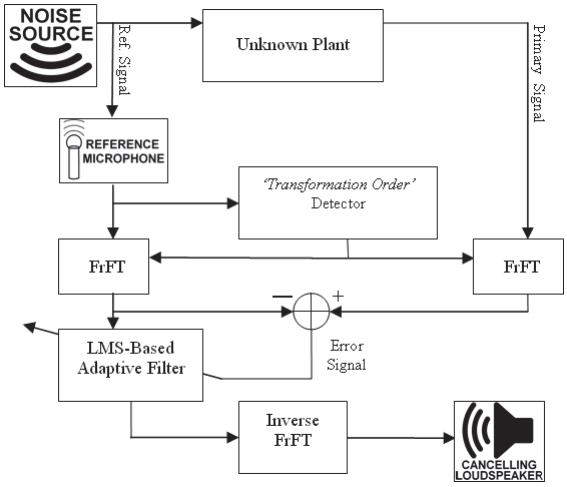

Fig. 8. The designed system model.

An LFM noise signal to be modeled by the fractional Fourier domain adaptive filter and its appropriately-ordered FrFT are shown in Fig.9(a) and (b). The chirp signal is transformed to a sinusoidal signal at the estimated transformation order of *a=1/3*. The input and output signals of the LMS-based adaptive filter in the fractional Fourier domain are given in Fig.(b) and (c). By taking the inverse FrFT of (c), time-domain filter output is obtained as shown in (d). The fractional Fourier domain error signals of both LMS and NLMS-based adaptive filters are plotted in Fig.10 (a) and (b). The adaptation step size μ can be chosen on the order of 10^{-1}. In the simulations, it is chosen as $\mu = 0.04$ in LMS and $\mu = 0.55$ in NLMS algorithm with $\alpha = 0$. In all of the simulations, adaptive filter length is chosen as *16* and among the two algorithms, NLMS performed better.

In the proposed fractional Fourier domain adaptive filtering scheme, the reference input $\mathbf{x}_p$ is transformed by the FrFT at the appropriate fractional order a so that the new input signal is

$$\mathbf{x}_p = \begin{bmatrix} x(n) \\ x(n-1) \\ \cdot \\ \cdot \\ x(n-p) \end{bmatrix} \rightarrow \mathbf{x}_{a,p} = \begin{bmatrix} x_a(n) \\ x_a(n-1) \\ \cdot \\ \cdot \\ x_a(n-p) \end{bmatrix}. \tag{11}$$

The reference and error signals are defined in the a^{th}-order fractional Fourier domain and represented by $d_a(n)$ and $e_a(n)$, respectively. The corresponding weight-update process of the transform-domain adaptive filter becomes

$$e_a(n) = d_a(n) - \mathbf{w}_a^T(n)\mathbf{x}'_{a,p}(n). \tag{12}$$

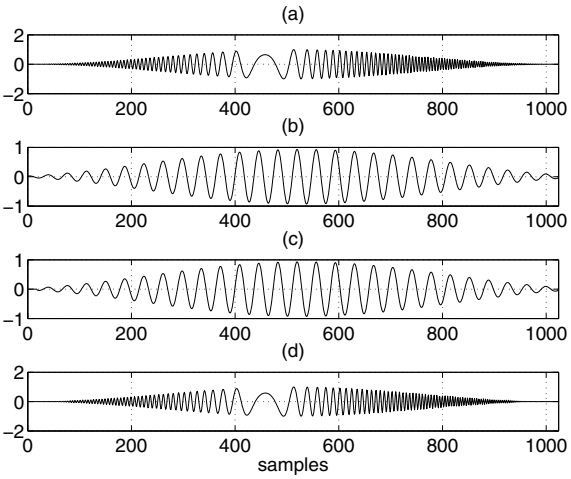

Fig. 9. An LFM signal, (b) its (1/3)rd order FrFT, (c) the output of the adaptive filter in FrFT domain and (d) the output of the adaptive filter in time domain by taking its inverse FrFT.

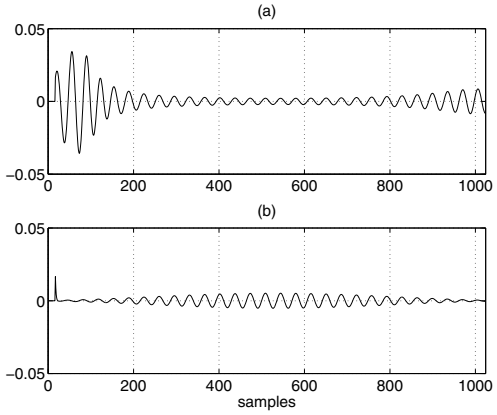

Fig. 10. Error signals in the fractional Fourier domain, by employing (a) LMS-based and (b) NLMS-based algorithms.

The tap-weights $\mathbf{w}_a(n)$ of the fractional Fourier domain adaptive filter are updated iteratively by

$$\mathbf{w}_a(n+1) = \mathbf{w}_a(n) + \mu \mathbf{x}'_{a,p}(n) e^*(n). \tag{13}$$

The FrFT parameter a should be estimated and kept updated during the adaptation process. FrFT-domain adaptation to an LFM signal is presented in Fig.12 by LMS and NLMS algorithms without introducing the secondary path effects *S(z)*. Fig.12(a) shows the chirp-type primary noise in time domain. This signal is transformed to a sinusoidal signal by taking FrFT at the appropriate order. Then, adaptation procedure is employed. Error plots of the LMS and NLMS algorithm in the fractional Fourier domain adaptation scheme are given in Fig.12(b) and (c), respectively. According to error signal of adaptive filters shown in Fig. 11 (b)-(c)

Fx-LMS Algorithm	
Input:	
Initialization vector:	$\mathbf{w}(n) = 0$
Input vector:	$\mathbf{x}(n)$
Desired output:	d(n)
Secondary path:	s(n)
Step-size parameter:	μ
Filter length:	M
Output:	
Filter output:	y(n)
Coefficient vector:	**w**(n+1)
Procedure:	
1) $y(n) = \mathbf{w}^H(n)\mathbf{x}(n)s(n)$	
2) $e(n) = d(n) - y(n)$	
3) $\mathbf{w}(n+1) = \mathbf{w}(n) + \mu e^*(n)\mathbf{x}(n)s(n)$	

Table 2. Fx-LMS Algorithm

and Fig. 12 (b)-(c) , it can be said that fractional Fourier domain adaptation performs well compared to time domain adaptation for chirp–type noise.
The fractional Fourier order parameter a is chosen as equal to the chirp rate, so the corresponding FrFT transforms the signal into a stationary signal. The simulation results present that fractional Fourier domain adaptive filtering is more successful at suppressing the undesired chirp-type noise compared to the time domain adaptation at the appropriate FrFT order.

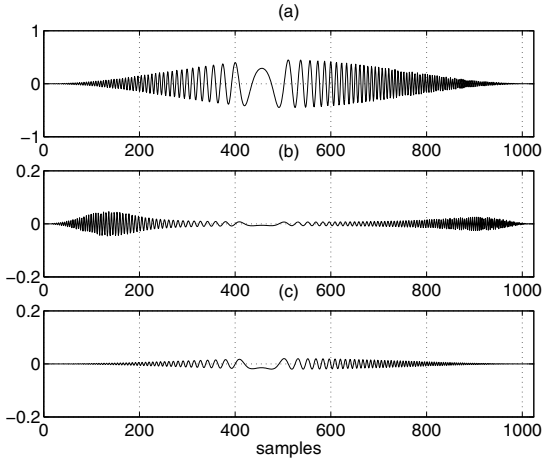

Fig. 11. (a) Primary noise in time domain, (b) LMS error, and (c) NLMS error by time domain adaptation.

The stability of the fractional Fourier domain LMS adaptation is assured by imposing limits on μ as

$$0 < \mu < 2/\lambda_m \tag{14}$$

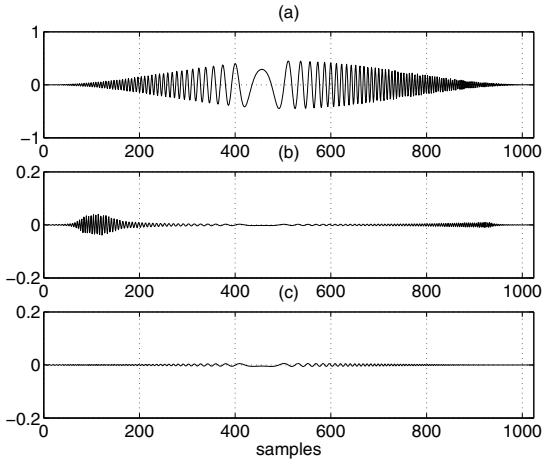

Fig. 12. (a) Primary noise in time domain, (b) LMS error, and (c) NLMS error by fractional Fourier domain adaptation.

where λ_m is the largest eigenvalue of the correlation matrix of the fractionally Fourier transformed input data. In case of the Fx-LMS algorithm, $\mathbf{x}'_{a,p}(n)$ is used as the filtered version of $\mathbf{x}_{a,p}(n)$ through $S(z)$. The observation period also depends on the computational power of the processor that operates the algorithm. IF estimation requires several times of FrFT algorithm giving rise to extra computational cost to the FrFT-domain adaptation.

Finally, the performance of the adaptive fractional Fourier domain LMS-based ANC is tested when the LFM noise signal is embedded into AWGN. Fig.13 presents error energy with respect to SNR, e.g., when SNR is 8 dB, the error energy in fractional Fourier domain adaptation scheme is less than 10^{-1}, whereas if the adaptation is realized in time, the error energy is greater than 1.

The fractional Fourier domain adaptation noticeably improves the system performance. The convergence analysis of the adaptive filtering schemes is realized for two alternative schemes. Fractional Fourier domain adaptive filtering scheme achieves faster adaptation compared to the time-domain adaptation algorithm as shown in Fig.14.

Fig.15 presents a real bat signal which has three different LFM components. Short–time Fourier transform (STFT) of this signal is given in Fig.16. The components of this signal are oriented along the same direction on the time-frequency plane and the FrFT transformation order is calculated as *a=0.0691* by the IF estimation algorithm proposed in (28). Error signals of time-domain and FrFT-domain adaptation are given in Fig. 17 (a) and (b), respectively. FrFT-domain adaptive filtering scheme gives better results compared to the time-domain adaptation.

[4] The authors wish to thank Curtis Condon, Ken White, and Al Feng from Beckman Institute of the University of Illinois for permission to use the bat data it in this paper.

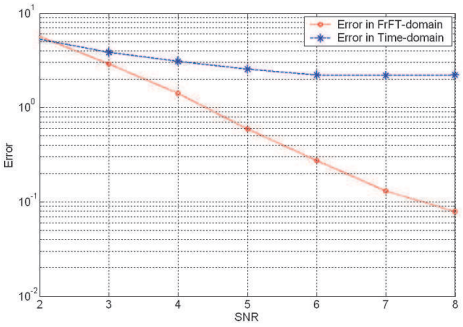

Fig. 13. Error energy in fractional Fourier and time-domain adaptation schemes with respect to SNR in AWGN.

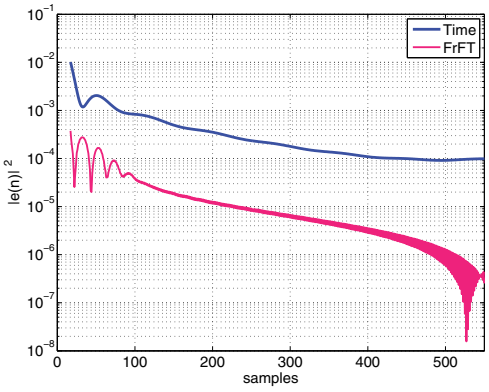

Fig. 14. Convergence analysis for both time and FrFT domain adaptive filtering.

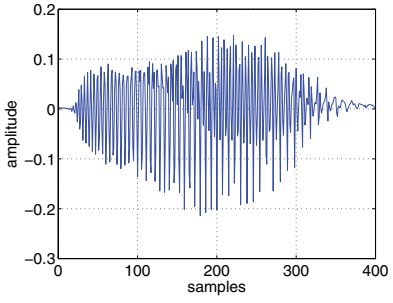

Fig. 15. Real bat echolocation signal which has multi-chirp components.

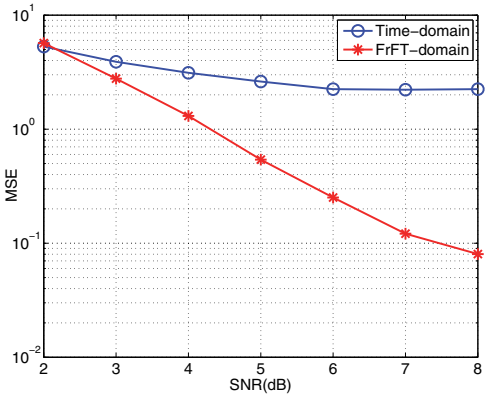

Fig. 16. STFT of the real bat signal.

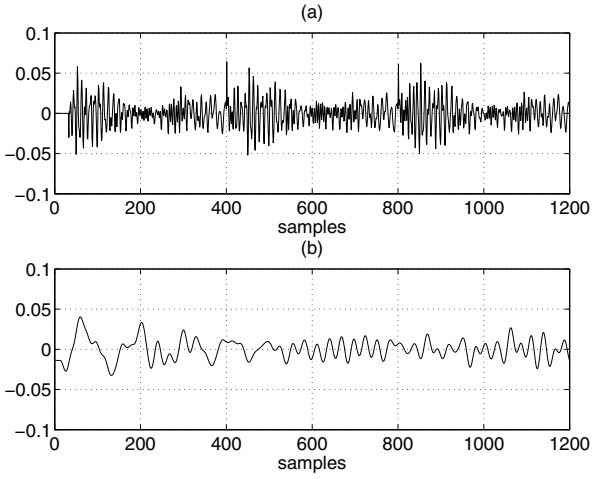

Fig. 17. (a) Error signal in Fx-NLMS algorithm by time-domain adaptation, (b) error signal in Fx-NLMS algorithm by fractional Fourier domain adaptation.

5. Conclusions

This chapter presents high-performance fractional Fourier domain adaptive filtering scheme for ANC systems. As a system parameter, the IF of the input chirp-type signal is estimated by searching the peak values of the modulus square of the FrFT. As noise signals originating from accelerating motion are chirp-type, such a fractional Fourier domain adaptive filtering approach avoids the difficulties of adaptation in a rapidly time-varying signal environment by transforming the signals to the appropriate fractional Fourier domain where the signals of interest become slowly time varying. Simulation results and error signals for mono-component chirp-type signals are compared in both time and fractional Fourier domains. It is evident that the total error quantity of adaptive filtering in fractional Fourier domain is significantly less than that of the time-domain adaptive filter.

6. Acknowledgements

This work is supported by the Scientific and Technological Research Council of Turkey, TUBITAK under the grant of Project No. 105E078.

7. References

[1] S. M. Kuo, "Active noise control: A tutorial review," Proc. IEEE, vol. 97, no. 6, (June, 1999), 943-973.
[2] C. Y. Chang and F. B. Luoh, "Enhancement of active noise control using neural-based filtered-X algorithm," Journal of Sound and Vibration, vol. 305, (2007), 348-356.
[3] G. Meng, X. Sun, S. M. Kuo, "Adaptive algorithm for active control of impulsive noise," Journal of Sound and Vibration, vol. 291, (2006),516-522.
[4] Y. L. Zhou, Q. Z. Zhang, X. D. Li, and W. S. Gan, "Analysis and DSP implementation of an ANC system using a filtered-error neural network," Journal of Sound and Vibration, vol. 285, (2005), 1-25.
[5] S. M. Kuo, S. Mitra, and W. S. Gan, "Active noise control system for headphone applications" IEEE Trans. on Control Syst. Tech., vol. 14, no. 2, (Mar., 2006), 331-335.
[6] W. S. Gan, R. G. Mitra, and S. M. Kuo,"Adaptive feedback active noise control headset: Implementation, evaluation and its extensions," IEEE Trans. on Consumer Electronics, vol. 51, no. 3, (Aug., 2005), 975-982.
[7] Z. Dayong and V. DeBrunner, "Efficient Adaptive Nonlinear Filters for Nonlinear Active Noise Control," IEEE Trans. on Circuits and Systems I, vol. 54, no. 3, (Mar., 2007), 669-681.
[8] C.Y. Chang and S.T. Li, "Active Noise Control in Headsets by Using a Low-Cost Microcontroller," IEEE Trans. on Industrial Electronics, vol. 58, no. 5, (May, 2011), 1936-1942.
[9] R. M. Reddy, I.M.S. Panahi, and R. Briggs, "Hybrid FxRLS-FxNLMS Adaptive Algorithm for Active Noise Control in fMRI Application," IEEE Trans. on Control Systems Technology, vol. 19, no. 2, (Mar., 2011), 474-480.
[10] B. J. Jalali-Farahani and M. Ismail, "Adaptive noise cancellation techniques in Sigma-Delta analog-to-digital converters," IEEE Trans. on Circuits and Systems I, vol. 54, no. 3, (Sep. 2007), 1891-1899.
[11] A. Goel, A. Vetteth, K. R. Rao, and V. Sridhar, "Active cancellation of acoustic noise using a self-tuned filter," IEEE Trans. on Circuits and Systems I, vol. 51, no. 11, (Mar., 2004),2148-2156.
[12] R.C. Selga and R.S.S. Peña, " Active Noise Hybrid Time-Varying Control for Motorcycle Helmets," IEEE Trans. on Control Systems Technology, vol. 18, no. 3, (May, 2010), 474-480.
[13] Z. Yuexian, C. Shing-Chow, and N. Tung-Sang, "Least mean M-estimate algorithms for robust adaptive filtering in impulse noise," IEEE Trans. on Circuits and Systems II vol. 47, no. 12, (Dec., 2000), 1564-1569.
[14] S. M. Kuo and D. R. Morgon, Active noise control: Algorithms and DSP implementations, New York: Wiley and Sons, 1996.
[15] W. S. Gan, Q. Z. Zhang, and Y. Zhou, "Adaptive recurrent fuzzy neural networks for active noise control," Journal of Sound and Vibration, vol. 296, (2006), 935-948.

[16] X. Liu X. Li, Q. Z. Zhang, Y. Zhou, and W. S. Gan, "A nonlinear ANC system with a SPSA-based recurrent fuzzy neural network controller," Lecture Notes in Computer Science, vol. 4491, 2007.
[17] Q. Z. Zhang and W. S. Gan, "Active noise control using a simplified fuzzy neural network," Journal of Sound and Vibration, vol. 272,(2004), 437-449.
[18] Q. Z. Zhang and W. S. Gan, A model predictive algorithm for active noise control with online secondary path modelling, Journal of Sound and Vibration, vol. 270, (2004), 1056-1066.
[19] M. Kawamata, M. T. Akhtar, M. Abe, and A. Nishihara, "Online secondary path modeling in multichannel active noise control systems using variable step size," Signal Process., vol. 88, (2008), 2019-2029.
[20] M. Joho and G. S. Moschytz, "Connecting partitioned frequency-domain filters in parallel or in cascade," IEEE Trans. on Circuits and Systems II, vol. 47, no. 8, (Aug., 2000), 685-698.
[21] S. Attallah, "The wavelet transform-domain LMS adaptive filter with partial subband coefficient updating," IEEE Trans. on Circuits and Systems II, vol. 53, no. 1, (Jan. 2006), 8-12.
[22] D. Veselinovic and D. Graupe, "A wavelet transform approach to blind adaptive filtering of speech from unknown noises," IEEE Trans. on Circuits and Systems II, vol. 50, no. 3,(Mar., 2003), 150-154.
[23] K. Mayyas and T. Aboulnasr, "Reduced-complexity transform-domain adaptive algorithm with selective coefficient update," IEEE Trans. on Circuits and Systems II, vol. 51, no. 3, (Mar., 2004), 132-142.
[24] S. Haykin, Adaptive Filter Theory, New Jersey: Prentice-Hall, 1996.
[25] H. M. Ozaktas, Z. Zalevski, and M. A. Kutay, "The Fractional Fourier Transform with Applications in Optics and Signal Processing," John Wiley and Sons, 2001.
[26] H. M. Ozaktas, O. Arıkan, M. A. Kutay, and G. Bozdagi, "Digital computation of the fractional Fourier transform," IEEE Trans. on Signal Process., 44(9), (Sept., 1996), 2141-2150.
[27] C. Candan, M. A. Kutay, and H. M. Ozaktas, "The discrete fractional Fourier transform", IEEE Trans. on Signal Process., 48(5), (May, 2000) 1329-1337,
[28] A. Serbes, L. Durak-Ata, "The discrete fractional Fourier transform based on the DFT matrix," Signal Process., 91 (3), (Mar., 2011), 571-581.
[29] A. W. Lohmann and B. H. Soffer, "Relationships between the Radon-Wigner and fractional Fourier transforms," J. Opt. Soc. Am. A, vol. 11, no. 6, (1994), 1798-1801.
[30] Q. Lin, Z. Yanhong, T. Ran, and W. Yue, "Adaptive filtering in fractional Fourier domain," IEEE Int. Symp. on Microw., Mape, (2), (Aug., 2005), 1033-1036.
[31] B. Boashash, "Estimating and interpreting the instantaneous frequency of a signal - Part II : Algorithms and applications," Proc. IEEE, vol. 80, no. 4, (Apr., 1992), 549-568.
[32] H. K. C. Kwok and D. L. Jones, "Improved instantaneous frequency estimation using an adaptive short-time Fourier transform," IEEE Trans. on Signal Process., vol. 10, no. 48, (Oct., 2000) 2964-2972.
[33] L. Durak and S. Aldırmaz, "Adaptive fractional Fourier domain filtering," Signal Processing, vol. 90, no. 4, (Apr., 2010), 1188-1196.

[34] C. F. Juang and C. T. Lin, "Noisy speech processing by recurrently adaptive fuzzy filters," IEEE Trans. on Fuzzy Systems, vol. 9 (Feb., 2001) 139-152.

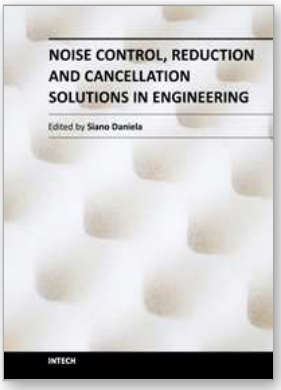

Noise Control, Reduction and Cancellation Solutions in Engineering

Edited by Dr Daniela Siano

ISBN 978-953-307-918-9
Hard cover, 298 pages
Publisher InTech
Published online 02, March, 2012
Published in print edition March, 2012

Noise has various effects on comfort, performance, and human health. For this reason, noise control plays an increasingly central role in the development of modern industrial and engineering applications. Nowadays, the noise control problem excites and attracts the attention of a great number of scientists in different disciplines. Indeed, noise control has a wide variety of applications in manufacturing, industrial operations, and consumer products. The main purpose of this book, organized in 13 chapters, is to present a comprehensive overview of recent advances in noise control and its applications in different research fields. The authors provide a range of practical applications of current and past noise control strategies in different real engineering problems. It is well addressed to researchers and engineers who have specific knowledge in acoustic problems. I would like to thank all the authors who accepted my invitation and agreed to share their work and experiences.

How to reference

In order to correctly reference this scholarly work, feel free to copy and paste the following:

Sultan Aldırmaz and Lütfiye Durak–Ata (2012). Adaptive Fractional Fourier Domain Filtering in Active Noise Control, Noise Control, Reduction and Cancellation Solutions in Engineering, Dr Daniela Siano (Ed.), ISBN: 978-953-307-918-9, InTech, Available from: http://www.intechopen.com/books/noise-control-reduction-and-cancellation-solutions-in-engineering/adaptive-fractional-fourier-domain-filtering

INTECH
open science | open minds

InTech Europe
University Campus STeP Ri
Slavka Krautzeka 83/A
51000 Rijeka, Croatia
Phone: +385 (51) 770 447
Fax: +385 (51) 686 166
www.intechopen.com

InTech China
Unit 405, Office Block, Hotel Equatorial Shanghai
No.65, Yan An Road (West), Shanghai, 200040, China
中国上海市延安西路65号上海国际贵都大饭店办公楼405单元
Phone: +86-21-62489820
Fax: +86-21-62489821